Wireless Multichannel Biopotential Recording Using an Integrated FM Telemetry Circuit

Pedram Mohseni, *Member, IEEE*, Khalil Najafi, *Fellow, IEEE*, Steven J. Eliades, and Xiaoqin Wang, *Member, IEEE*

***Abstract*—This paper presents a four-channel telemetric microsystem featuring on-chip alternating current amplification, direct current baseline stabilization, clock generation, time-division multiplexing, and wireless frequency-modulation transmission of microvolt- and millivolt-range input biopotentials in the very high frequency band of 94–98 MHz over a distance of ~ 0.5 m. It consists of a 4.84-mm^2 integrated circuit, fabricated using a 1.5-μm double-poly double-metal n-well standard complementary metal–oxide semiconductor process, interfaced with only three off-chip components on a custom-designed printed-circuit board that measures $1.7 \times 1.2 \times 0.16$ cm^3, and weighs 1.1 g including two miniature 1.5-V batteries. We characterize the microsystem performance, operating in a truly wireless fashion in single-channel and multichannel operation modes, via extensive benchtop and *in vitro* tests in saline utilizing two different micromachined neural recording microelectrodes, while dissipating ~ 2.2 mW from a 3-V power supply. Moreover, we demonstrate successful wireless *in vivo* recording of spontaneous neural activity at 96.2 MHz from the auditory cortex of an awake marmoset monkey at several transmission distances ranging from 10 to 50 cm with signal-to-noise ratios in the range of 8.4–9.5 dB.**

***Index Terms*—*In vivo* neural recording, multichannel biotelemetry, neural prostheses, wireless frequency-modulation (FM) microsystem.**

I. Introduction

WIRELESS transmission of biological data with radio waves has been widely utilized in monitoring biopotentials such as electrocardiograms [1], [2], electromyograms [3], [4], and electroencephalograms [5]. Kim *et al.* have proposed a discrete wireless biotelemetry system using a frequency modulation (FM) stereo method to monitor the respiration and heart-sound signals in exercising rehabilitation patients [6]. Sears *et al.* have developed a microcontroller-based biotelemetric heart-valve monitor using commercially available amplifiers and signal converters [7]. These large-scale board-level discrete designs have successfully proved the feasibility of single-channel or multichannel signal acquisition, conditioning, transmission to a remote receiver, and reconstruction of the original waveforms with reasonable accuracy.

In the realm of neuroscience, rapid progress in the field of micromachined recording electrodes has remarkably benefited neurophysiology over the past few decades. Researchers around the world have utilized microelectro-mechanical-system (MEMS) technology to fabricate submillimeter-scale recording probes that allow long-term, reliable, and stable recording of neural signals from the central or peripheral nervous system [8]–[11]. Telemetry systems are becoming as indispensable as microelectrode arrays due to their capability of simultaneously recording and transmitting neural signals, of eliminating electrical artifacts due to the movement of cables in tethered measurements, and of avoiding the risk of skin irritation or infection caused by percutaneous leads in bioimplantable microsystems.

Developing telemetry systems to broadcast neural activity is challenging mainly due to the fact that an extracellular single-unit neural action potential is a spike of 50–500 μV in amplitude and 0.1–6 kHz in bandwidth [12]. Eichenbaum *et al.* and Pinkwart *et al.* have reported pioneering telemetry systems for single-neuron recording and wireless brain stimulation [13], [14]. Over the years, continuous improvements in the manufacturing of electrical components (e.g., surface-mount devices) and novel design methodologies in application-specific integrated circuits (ASICs) have resulted in robust multichannel telemetry microsystems suitable for a vast majority of industrial and research activities [15]–[25]. Nieder reported a miniature radio transmitter for simultaneous recording of multiple single-neuron signals in behaving owls [15]. This discrete two-channel system weighs 3.1 g (without batteries), and measures $2.5 \times 1 \times 0.5$ cm^3. Takeuchi *et al.* reported a radio-frequency (RF) telemetry system for neural recording in freely moving insects interfacing with shape memory alloy (SMA) microelectrodes [16]. This discrete single-channel system has a relatively high power consumption of 10 mW resulting in a lifetime of only 30 min. Obeid *et al.* have reported a 16-channel wearable telemetry system for single-unit neural recording that measures $5.1 \times 8.1 \times 12.4$ cm^3, weighs 235 g, and dissipates 4 W from rechargeable lithium-ion batteries [17]. Clearly, all these discrete board-level designs with commercially available electrical components have either prohibitively large dimensions and weight or high power consumption that makes them impractical for general-purpose low-power applications. Song *et al.* have reported a single-chip system for the acquisition, digitization, and wireless telemetry of biological signals [18]. This single-channel system consumes 10 mW of power from a 2.5-V supply in a standard 2-μm digital CMOS process. Kim *et al.* reported an integrated wireless telemetry system in the 902–928 MHz ISM band consuming close to

Manuscript received December 8, 2005; revised April 5, 2005; accepted May 13, 2005. The biological experiments were conducted in the Laboratory of Auditory Neurophysiology at Johns Hopkins University (supported under the National Institutes of Health Grant R01-DC005808). This work was supported under the National Institutes of Health Grant R01-DC04198-01. This work also made use of Engineering Research Center Shared Facilities supported by the National Science Foundation under Award EEC-0096866.

P. Mohseni and K. Najafi are with the Center for Wireless Integrated MicroSystems (WIMS), Department of Electrical Engineering, University of Michigan, Ann Arbor, MI 48109-2122 USA (e-mail: pmohseni@umich.edu; najafi@umich.edu).

S. J. Eliades and X. Wang are with the Department of Biomedical Engineering, The Johns Hopkins University School of Medicine, Baltimore, MD 21205 USA (e-mail: seliades@jhu.edu; xiaoqin.wang@jhu.edu).

Digital Object Identifier 10.1109/TNSRE.2005.853625

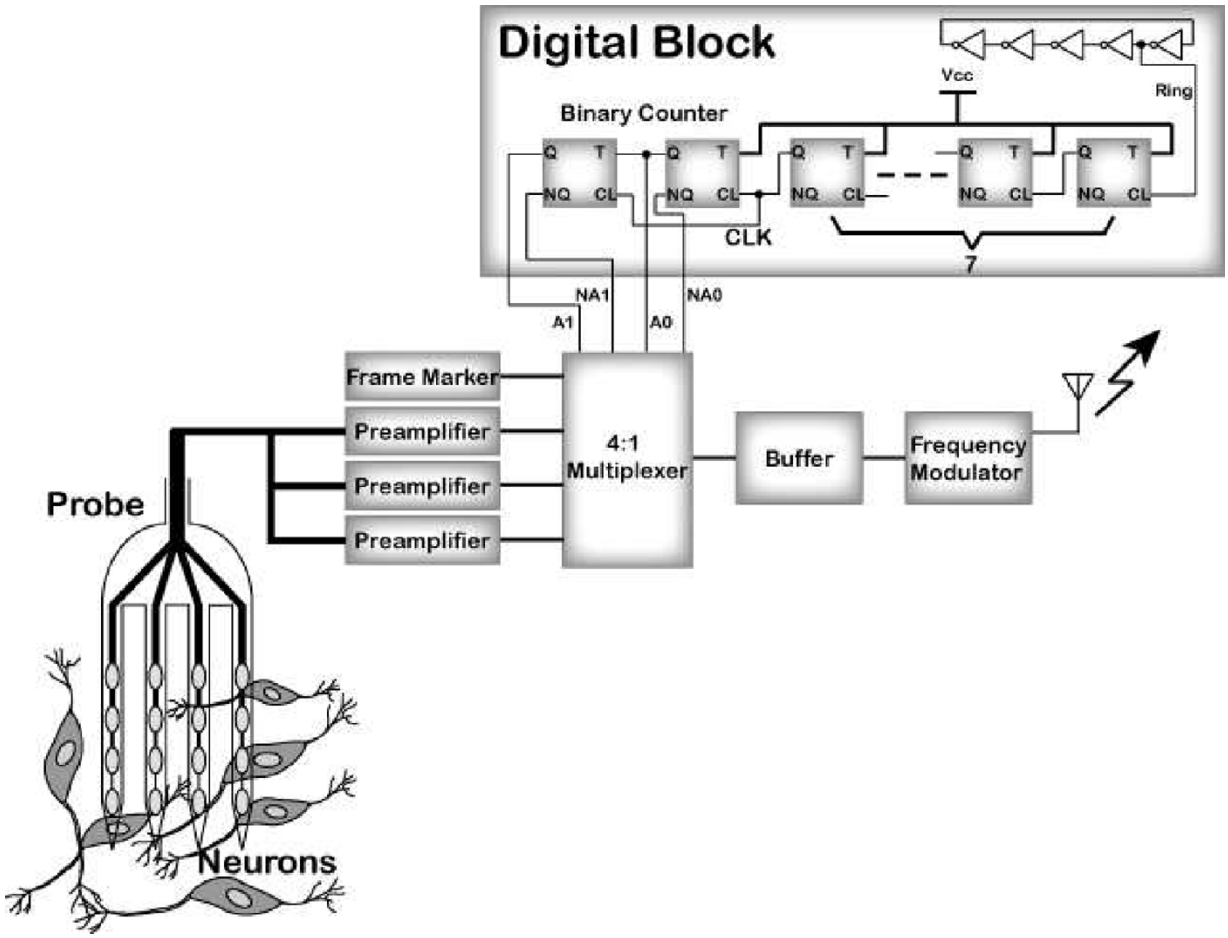

Fig. 1. Block diagram of the four-channel wireless FM biopotential recording microsystem.

50 mW of power in a 0.18-μm copper CMOS process [19]. Parramon *et al.* have reported an implantable inductively powered two-channel recording microsystem fabricated in a 2.5-μm BiCMOS process with a current consumption of 4.5 mA at 5 V [20]. Irazoqui-Pastor *et al.* have reported *in vivo* electroencephalogram (EEG) recordings from untethered rodents using an inductively powered implantable wireless neural recording device [21]. This single-channel system operates at 3.2 GHz, has a power consumption of 5–8 mW, and is fabricated in a 0.35-μm CMOS process. DeMichele *et al.* reported a 16-channel integrated wireless biotelemetry system dissipating 18 mW of power from a 4.75-V power supply in a 1.5-μm BiCMOS process [22]. Johannessen *et al.* have reported a microelectronic pill utilizing system-level integration of microsensors and integrated circuits in a four-channel recording device fabricated in a 0.6-μm CMOS process that consumes 12.1 mW of power, measures 5.5×1.6 cm^2, and weighs 13.5 g including two silver-oxide batteries [23]. Finally, Yu *et al.* have reported an eight-channel inductively powered wireless bioimplantable microsystem, which consists of two separate chips, consumes 12.7 mW, and weighs 1.2 g [24]. Biomedical telemetry systems have evolved in the past decades from simple single-channel devices into more complex multichannel systems. Utilizing novel methodologies in low-power low-noise ASIC design has brought about many of these changes. In this paper, we report on the design, implementation, testing, and performance characterization of miniature single-channel and multichannel wireless frequency-modulated systems for biopotential recording applications, which combine signal amplification, direct current (dc) baseline stabilization, monolithic clock generation, time-division multiplexing, and wireless transmission of microvolt- and millivolt-range input biopotentials, all on the same silicon substrate with substantially lower power dissipation per number of recording channels compared to all the aforementioned previous work [26]. Section II presents the individual building blocks of the microsystem together with their measured performance, while Section III reports the full system wireless measurement results. Finally, Section IV draws some conclusions from this work.

II. Microsystem Architecture

Fig. 1 shows the block diagram of the four-channel wireless FM biopotential recording microsystem. Three on-chip preamplifiers amplify the recorded signals, which are then sequentially sampled, multiplexed in time, and buffered for transmission over an RF link to the outside world. The analog multiplexer is controlled by an on-chip-generated clock signal that sets the sampling rate. A fourth sample, a reference dc bias referred to as a frame marker, is also multiplexed with the three data channels so that the on-chip clock frequency can be regenerated off-chip by the external receiver system for demultiplexing. Fig. 2 shows the transistor-level circuit schematic of one recording channel in the microsystem.

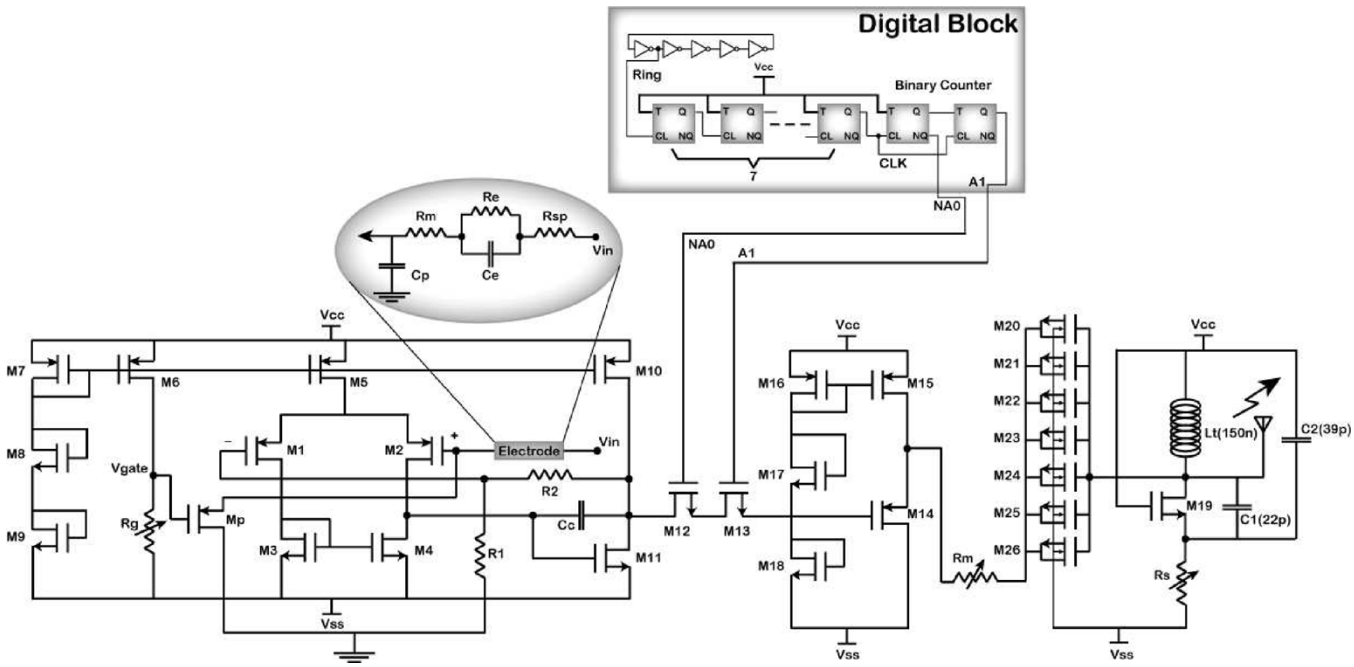

Fig. 2. Transistor-level circuit schematic of one recording channel.

A. Preamplifier

We have previously reported a fully integrated bandpass neural recording preamplifier with dc input stabilization that provides a stable alternating current (ac) gain of 39.3 dB at 1 kHz in a closed-loop resistive-feedback configuration [27]. A subthreshold p-type metal oxide semiconductor (pMOS) input transistor $M_{\rm p}$ in conjunction with the electrode capacitance $C_{\rm e}$ is used to clamp the large and random dc open-circuit potentials that normally exist at the electrode–electrolyte interface. The low cutoff frequency of the preamplifier is programmable up to 50 Hz, while its high cutoff frequency is measured to be 9.1 kHz. The tolerable dc input range is measured to be at least ± 0.25 V with a dc rejection factor of at least 29 dB.

It dissipates 115 μW from a 3-V supply, occupies a die area of 0.107 mm^2, and has a total measured input-referred noise voltage of 7.8 $\mu V_{\rm rms}$ in the frequency range of 0.1–10 kHz. By adjusting the values of the gain-setting feedback resistors in a modified design employed as the analog front-end in this work, we have also achieved a stable ac gain of 43.7 dB at 1 kHz, while dissipating 90 μW from a 3-V power supply. The new total input-referred noise voltage in the frequency range of 0.1–10 kHz is measured to be 7.1 $\mu V_{\rm rms}$.

B. Digital Block

The clock-generation circuitry consists of a five-stage ring oscillator followed by a seven-stage chain of T flip-flops. The ring oscillator generates a sinusoidal output at $\sim$ 8.6 MHz. The seven-stage T flip-flop chain divides this frequency down to $\sim$ 70 kHz, generating the clock signal for the two-bit binary counter to control the 4:1 analog multiplexer (see Fig. 2). Since there are four logic states in the binary counter corresponding to the number of input channels, there is no unused state. Hence, regardless of what initial state the counter is in when the power is turned on, the frame marker level will always indicate the start of the first sampling frame after a maximum of three clock cycles. The digital block dissipates ~ 516 μW from a 3-V power supply, and occupies a die area of 0.815 mm^2.

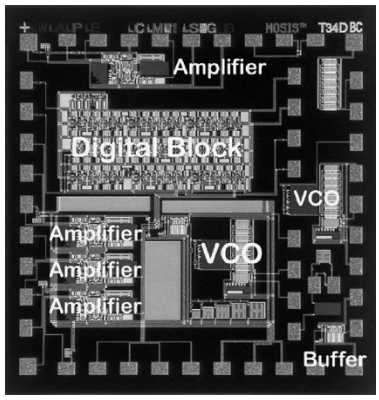

Fig. 3. Microphotograph of the fabricated chip.

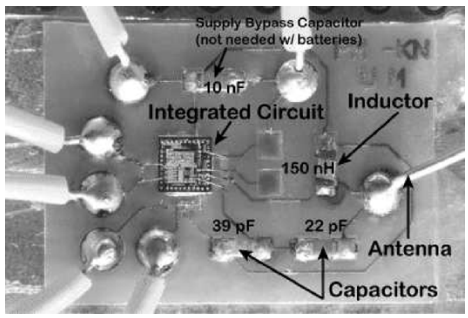

Fig. 4. Photograph of a fully assembled recording system.

C. Multiplexer/Buffer

After on-chip amplification and dc baseline stabilization, the three recorded signals are multiplexed in time with the frame

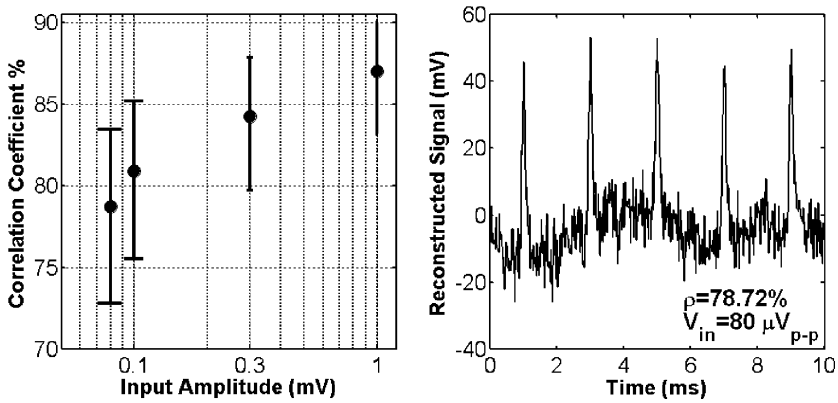

Fig. 5. Measured I/O correlation coefficients versus input amplitude after single-channel wireless transmission at 96.5 MHz (left) and wireless recording of 80-$\mu V_{p\text{-}p}$ simulated neural spikes (right). All five input spikes were captured during a 10-ms time span. Error bar represents a 95% confidence interval around the corresponding correlation coefficient.

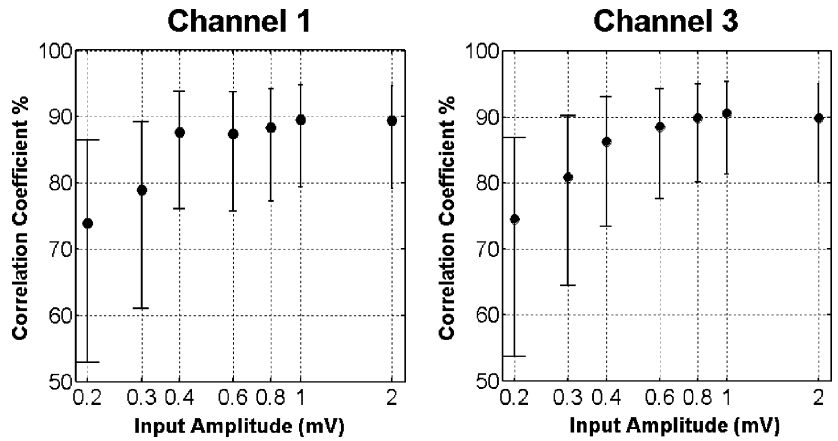

Fig. 6. Measured I/O correlation coefficients per channel versus input amplitude after multichannel wireless transmission at 97.8 MHz.

marker. The n-type metal–oxide–semiconductor (nMOS) gates, controlled by the output signals of the logic-control circuitry, pass the amplified signals in sequence for one clock period. The frame marker is similarly connected to the multiplexed shared lead during the fourth time interval. A wide-band source-follower amplifier then buffers the multiplexed signal before transmission to the outside world. The buffer has a measured gain of 0.92, very high input impedance, low output impedance of 1.8 $k\Omega$, a power dissipation of 113 μW from a 3-V power supply, and a die area of 0.025 mm^2.

D. Frequency Modulator

We have previously reported a low-phase-noise hybrid-LC-tank analog frequency modulator for wireless biotelemetry employing programmable-in-size on-chip inversion-mode nMOS varactors as the frequency tuning element [28]. It operates within the frequency band 88–108 MHz, set aside by the U.S. Federal Communications Commission (FCC) for unlicensed custom-built telemetry radiators for experimentation in educational institutes [29]. Inductance–capacitance (*LC*)-tank components (1 inductor and 2 capacitors) are external surface-mount devices that are wire bonded to the integrated circuit on a custom-designed printed circuit board (PCB). We have demonstrated that if the large-amplitude oscillation effect on the integrated tank varactor is overlooked at the design stage, it will lead to a gross overestimation of the *destination* signal-to-noise ratio (SNR) (i.e., the average signal-to-noise power ratio at the receiver output), which quantifies the received signal quality in an FM biotelemetry system. The frequency modulator occupies a die area of 0.21 mm^2, and achieves a measured gain factor of 1.21 MHz/V in the midrange of the tuning voltage and a phase noise of -88.6 dBc/Hz at 10-kHz offset from the 95.1-MHz carrier while dissipating 1.48 mW from a 3-V power supply leading to a figure of merit (FOM) of -166.5 dBc/Hz.

III. Wireless Measurement Results

Prototype chips were fabricated using the AMI 1.5-μm double-poly double-metal n-well CMOS process. Fig. 3 shows a microphotograph of the fabricated chip. The 4.84-mm^2 ICs were attached to a custom-designed PCB using conductive epoxy (P-10) after soldering the voltage-controlled oscillator's (VCOs) three off-chip components in place. Chip attachment was also preceded by soldering six short flexible wires to the PCB for ± 1.5-V power supply, ground connection, and three input lines. The chip was then wire bonded to the PCB with 11 aluminum wire bonds. A short ($\sim$ 2 cm) wire monopole antenna was also soldered in place to radiate the FM signal. A fully assembled system, shown in Fig. 4, measured $1.7 \times 1.2 \times 0.16$ cm^3, and weighed 1.1 g including two miniature batteries. Utilizing smaller-sized off-chip components

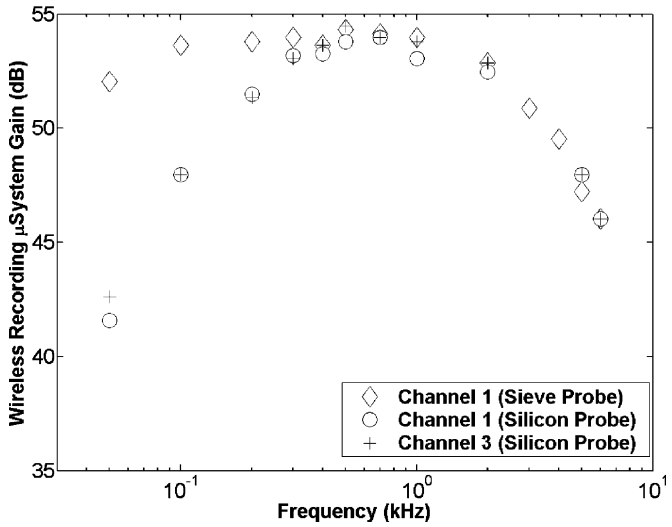

Fig. 7. Recording microsystem bandpass frequency response per channel after wireless *in vitro* recording from saline with the telemetry chip interfaced with two different micromachined neural recording microelectrodes.

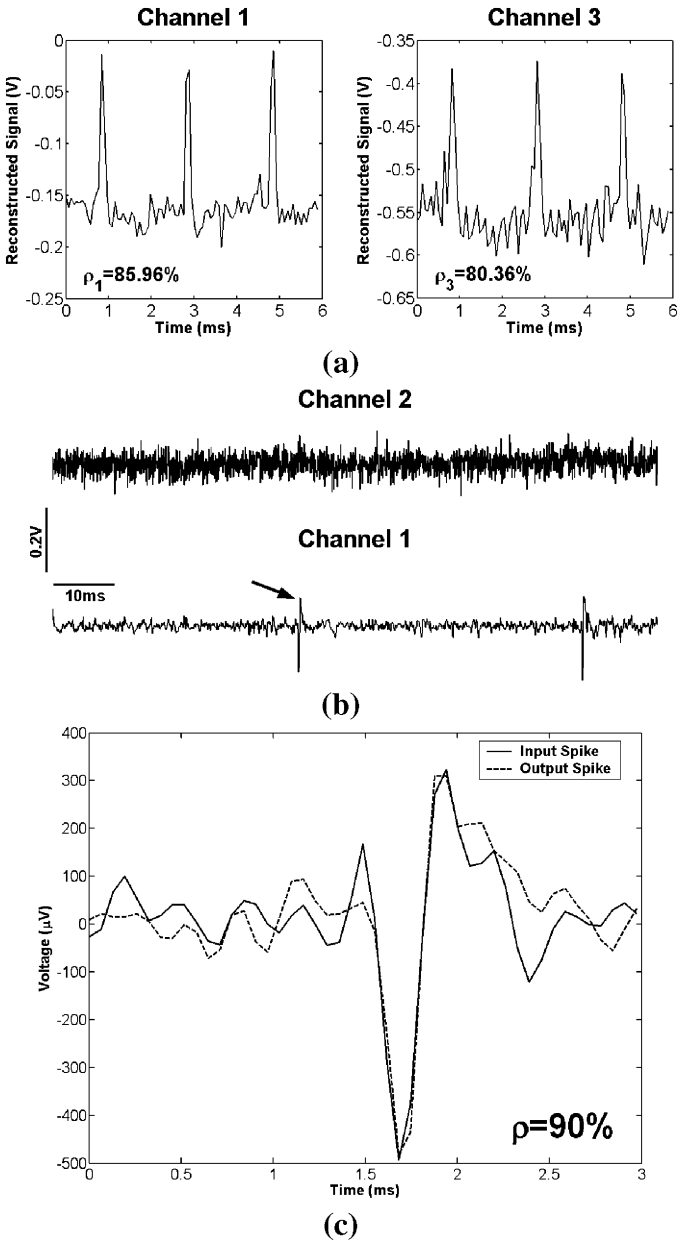

Fig. 8. (a) Simultaneous wireless *in vitro* recording of 500-Hz, 400-$\mu V_{p\text{-}p}$ simulated neural spikes on a 50-mV dc level from saline with the telemetry chip interfaced with a 700-μm^2 iridium recording site on a silicon neural recording microprobe. Measured I/O correlation coefficients for the reconstructed signals were $> 80\%$. (b) Simultaneous wireless *in vitro* recording of prerecorded neural activity on channel 1 interfaced with a 3000-μm^2 gold recording site on a polyimide sieve electrode with channel 2 grounded at the input. Duration of time axis is 100 ms. (c) Expanded view of the input-referred wirelessly recorded output spike on channel 1 superimposed on the corresponding extracellular neural spike input to the microsystem.

together with a thinner double-sided PCB can further decrease the total volume to 10 mm^3.

Individual preamplifier, buffer, and VCO test structures were placed along the periphery of the die near the bond pads. These test structures were wire bonded to a 24-pin hybrid platform package, and were connected to each other off-chip to form a single recording channel. Fig. 5 depicts the measured I/O correlation coefficients with a simulated neural spike train input (8-kHz bandwidth) for four different values of input amplitude after wireless transmission at 96.5 MHz where the error bar represents a 95% confidence interval around the corresponding correlation coefficient. It also shows the *single-channel* wireless reconstruction of 500-Hz, 80-$\mu V_{p\text{-}p}$ neural spikes with a measured I/O correlation coefficient of $\sim 79\%$. The single-channel wireless microsystem fully captured the five input spikes over a 10-ms time span while dissipating ~ 1.66 mW from a 3-V power supply.

To fully characterize the performance of the telemetry system in *multichannel* operation mode, extensive benchtop and *in vitro* tests in saline were performed using two different micromachined neural recording microelectrodes. The polyimide sieve electrode was 30 mm in length, and had three electroplated gold recording sites with an average impedance magnitude of 175 k$\Omega\angle -68°$ at 1 kHz [30] whereas the penetrating silicon electrode was 5 mm in length, and had 16 iridium recording sites with an average impedance magnitude of 412 k$\Omega\angle -56°$ at 1 kHz [31].

We first applied a 500-Hz simulated neural spike train to input channels 1 and 3, with channel 2 grounded at the input. We varied its amplitude in the range of 0.2–2 $mV_{p\text{-}p}$, and measured the I/O correlation coefficients per channel after wireless transmission at 97.8 MHz, as shown in Fig. 6. Measured values for the reconstructed data channels were in very good agreement with each other. Correlation coefficients in the range of $\sim$ 74%–90% were obtained over a wireless transmission distance of ~ 0.25 m.

To measure the frequency response of the wireless recording microsystem, we interfaced our telemetric chip with the silicon microelectrode for simultaneous multichannel wireless *in vitro* recording. We applied a 1-$mV_{p\text{-}p}$ sinusoidal signal with a 50-mV dc level to saline, varied its frequency in the range of 0.05–7 kHz, and measured the overall gain of the microsystem versus frequency for recording channels 1 and 3, as shown in Fig. 7. Measured values for the two reconstructed channels were again in excellent agreement with each other. The wireless microsystem had a total ac gain of > 53 dB at 1 kHz. The front-end preamplifiers rejected the dc frequency component in the input, and amplified only the ac part. The low-frequency roll-off in gain shown in Fig. 7 is a result of the dc baseline stabilization

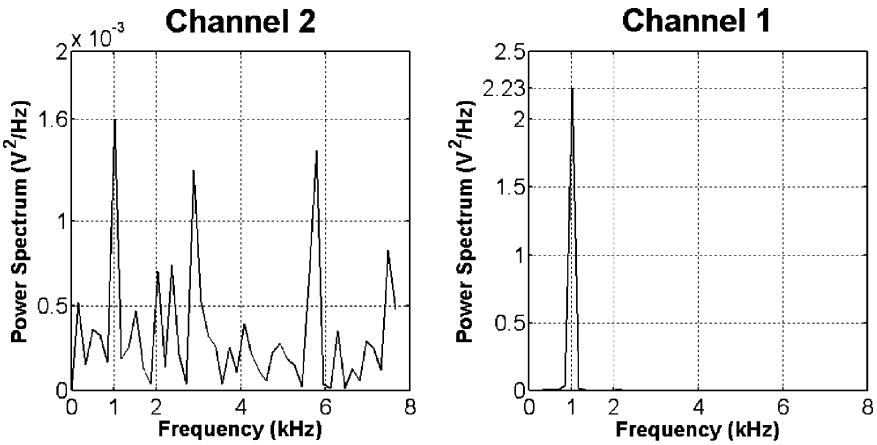

Fig. 9. Measured power spectrum of the simultaneously received signals when a 1-kHz sinusoidal waveform was applied to channel 1 from saline via a polyimide sieve electrode, while channel 2 was grounded at the input. Difference in the received signal power at 1 kHz was ~ 31.44 dB, which would amount to $\sim 2.68\%$ crosstalk between the two adjacent channels.

TABLE I
WIRELESS BIOPOTENTIAL RECORDING MICROSYSTEM PERFORMANCE COMPARISON

	This Work		[15]	[16]	[20]	[21]	[23]
Data Channels	1	3	2	1	2	1	4
Telemetry Freq.	94-98 MHz		88-108 MHz	80-90 MHz	30 MHz	3.2 GHz	20-40 MHz
Comm. Scheme	TDM/Analog FM		FM Stereo	Analog FM	BPSK	Analog FM	TDMA/FSK
Power Supply	±1.5 V		±1.4 V	3 V	5 V	2-3.2 V	3.1 V
Power Diss.	1.66 mW	2.2 mW	-	10 mW	22.5 mW	5-8 mW	12.1 mW
Trans. Range	0.5 m		a few meters	~16 m	1 cm	0.5 m	1 m
Dimensions	$1.7 \times 1.2 \times 0.16$ cm^3		$2.5 \times 1 \times 0.5$ cm^3	1.5×0.8 cm^2	$1.1 \times 1.1 \times 0.7$ cm^3	$0.5 \times 0.5 \times 1$ cm^3	1.6×5.5 cm^2
Total Weight	1.1 g		>3.1 g	>0.1 g	-	-	13.5 g
External Comp.	3		28	19	8	0	8
Technology	1.5µm CMOS		-	-	2.5µm BiCMOS	0.35µm CMOS	0.6µm CMOS
Implementation	Single Chip		Discrete	Discrete	Single Chip	Single Chip	Hybrid
Publication Year	2004		2000	2004	1997	2003	2004

mechanism in the preamplifiers. Fig. 8(a) depicts simultaneous two-channel wireless *in vitro* recording of 500-Hz, 400-$\mu V_{p\text{-}p}$ simulated neural spikes with a 50-mV dc level from saline using the silicon microprobe. The reconstructed data channels had an I/O correlation coefficient of $> 80\%$, and the three input spikes were fully captured on each channel during a 6-ms time span.

We then interfaced our telemetric chip with the polyimide sieve electrode. With channels 2 and 3 grounded, we measured the frequency response of channel 1, as also shown in Fig. 7. The measured response with the sieve electrode was in excellent agreement with that with the silicon probe, except that the low-frequency roll-off in gain occurred at a lower frequency. This was due to the fact that the effective area of the recording sites on the sieve probe ($\sim 3000\ \mu m^2$) was much larger than that on the silicon probe (700 μm^2) resulting in a higher electrode capacitance for the sieve probe, which, in turn, would result in a lower cutoff frequency in the front-end preamplifiers due to the dc baseline stabilization mechanism employed in this work [27].

Fig. 9 shows the measured power spectrum of the wirelessly received signals on data channels 1 and 2 when a 1-kHz, 1-$mV_{p\text{-}p}$ sinusoidal waveform on a 50-mV dc level was applied to channel 1 from saline via the sieve electrode with channel 2 grounded at the input. The difference in the received signal power at 1 kHz was ~ 31.44 dB, which would amount to $\sim 2.68\%$ crosstalk between the two adjacent channels.

We also applied a 100-ms snapshot of prerecorded neural activity containing two distinguishable submilivolt extracellular neural action potentials on a 50-mV dc level to saline. The activity was evoked by an acoustic white noise burst from the inferior colliculus of an anesthetized guinea pig. A dc level of ± 50 mV is typical for the dc electrochemical potentials at the electrode–electrolyte interface for gold recording sites in buffered saline [27]. Fig. 8(b) depicts the simultaneously received data channels at 97.8 MHz while channel 1 was interfaced with the micromachined sieve electrode and channel 2 was grounded at the input. A digital Chebyshev type-II infinite impulse response (IIR) bandpass filter (0.3–4 kHz) was applied to the received data post-acquisition. The two neural spikes were fully captured on channel 1, while no significant activity could be observed on channel 2. Fig. 8(c) shows an expanded view of the input-referred wirelessly recorded output spike, denoted by an arrow in Fig. 8(b), superimposed on the corresponding input neural action potential. The measured correlation coefficient between the two waveforms was $\sim 90\%$. In all these experiments, the telemetric microsystem was powered with two batteries drawing $\sim 732\ \mu A$ from ~ 3 V leading to a total power dissipation of ~ 2.2 mW. Table I tabulates the overall perfor-

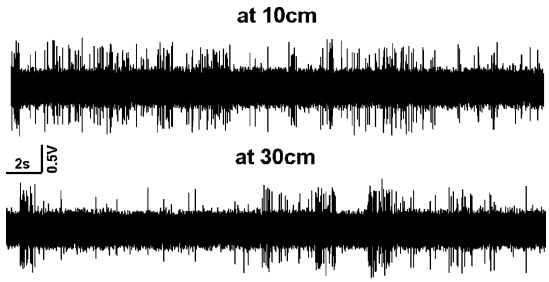

Fig. 10. Wireless *in vivo* recording of spontaneous neural activity in the nonprimary auditory cortex of an awake marmoset monkey at 96.2 MHz at 10 and 30 cm away from the transmitter. Measured SNRs were 9.5 and 9 dB, respectively. Duration of time axis is 30 s.

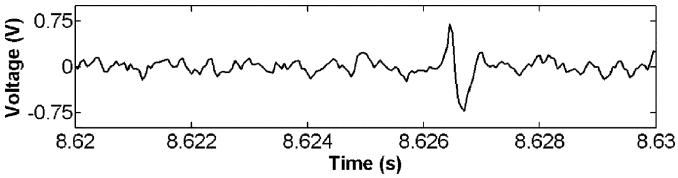

Fig. 11. Expanded view of a representative single spike recorded *in vivo*. Signal was transmitted wirelessly over a distance of 10 cm between the transmitter and receiver.

mance characteristics of the wireless recording microsystem, and compares them with those in recent published work.

A. Biological Tests

Biological experiments were conducted on an awake marmoset monkey (*Callithrix Jacchus*) [32] that was chronically implanted with a microelectrode array made up of 16 sharp tungsten electrodes with an average impedance magnitude of 0.6–0.8 $\mathrm{M}\Omega$ at 1 kHz. Spontaneous neural activity was wirelessly recorded from the nonprimary auditory cortex at different transmission ranges in a single-channel operation mode. Fig. 10 depicts the wirelessly recorded *in vivo* data at 96.2 MHz obtained at 10 and 30 cm away from the transmitter with post-acquisition bandpass filtering applied (0.3 to 4.5 kHz). In addition to ~ 50.1 dB of gain provided by the on-chip circuitry, an off-chip gain of ~ 20 dB was applied *after* frequency demodulation at the receiver for digitization and capturing of the neural data. SNRs of 9.5, 9, and 8.4 dB were achieved at 10, 30, and 50 cm away, respectively. Measured SNR in a wired case using rack-mounted recording equipment was 13.9 dB.

Finally, Fig. 11 shows an expanded view (10-ms time span) of a wirelessly recorded *in vivo* spike at 10 cm away from the transmitter.

IV. Conclusion

In this paper, we reported on the design, implementation, and testing of a single-channel and multichannel telemetric microsystem combining ac amplification, dc input stabilization, clock generation, time-division multiplexing, and wireless FM transmission of three input biopotentials. All of this functionality was provided by one silicon chip, fabricated using the AMI 1.5-μm 2P/2M n-well CMOS process, interfaced with only three off-chip components on a custom-designed PCB, which measured $1.7 \times 1.2 \times 0.16$ cm^3, weighed 1.1 g including two miniature batteries, and dissipated ~ 2.2 mW from a 3-V power supply. Measured performance of the individual circuit blocks, as well as the performance characteristics of the entire microsystem operating in a truly wireless fashion were reported after extensive benchtop and *in vitro* tests in saline using a polyimide nerve-regeneration sieve electrode and a penetrating silicon microelectrode array. Moreover, spontaneous neural activity was wirelessly recorded in an awake marmoset monkey at distances up to 0.5 m away with SNR > 8.4 dB using the telemetry chip.

Acknowledgment

The authors would like to thank Prof. M. F. Schmidt and Dr. P. Nealen from the Department of Biology, University of Pennsylvania, for their collaboration and helpful discussions that made this work possible. The design, implementation, testing, and characterization of the telemetric device were performed at the University of Michigan.

References

[1] J. H. Filshie, I. J. H. Duncan, and J. S. B. Clark, "Radiotelemetry of avian electrocardiogram," *Med. Biol. Eng. Comput.*, vol. 18, pp. 633–637, Sep. 1980.

[2] T. B. Fryer, H. Sandler, W. Freund, E. P. McCutcheon, and E. L. Carlson, "A multichannel implantable telemetry system for flow, pressure, and ECG measurements," *J. Appl. Physiol.*, vol. 39, no. 2, pp. 318–326, Aug. 1975.

[3] M. Steyaert, S. Gogaert, T. Van Nuland, and W. Sansen, "A low-power portable telemetry system for eight-channel EMG measurements," in *Proc. Annu. Int. IEEE-EMBS Conf.*, vol. 13, 1991, pp. 1711–1712.

[4] M. Marques and B. Dutourne, "Implantable telemetry system for long-term EMG," *Biotelemetry*, vol. 4, pp. 28–33, 1977.

[5] R. Wertz, G. Maeda, and T. J. Willey, "Design for a micropowered multichannel PAM/FM biotelemetry system for brain research," *J. Appl. Physiol.*, vol. 41, no. 5, pp. 800–805, Nov. 1976.

[6] Y. Kim and J. M. Cho, "Development of wireless biotelemetry system using FM stereo method for exercising rehabilitation patients," in *Proc. 23rd Annu. Int. IEEE-EMBS Conf.*, vol. 4, Istanbul, Turkey, Oct. 25–28, 2001, pp. 3338–3340.

[7] J. R. Sears and J. F. Naber, "Development of a biotelemetric heart valve monitor using a 2.45 GHz transceiver, microcontroller, A/D converter, and sensor gain amplifiers," in *Proc. 1st Joint EMBS/BMES Conf.*, Atlanta, GA, Oct. 13–16, 1999, p. 794.

[8] Q. Bai, K. D. Wise, and D. J. Anderson, "A high-yield micro-assembly structure for three-dimensional microelectrode arrays," *IEEE Trans. Biomed. Eng.*, vol. 47, no. 3, pp. 281–289, Mar. 2000.

[9] T. Akin, K. Najafi, R. Smoke, and R. Bradley, "A micromachined silicon sieve electrode for nerve regeneration applications," *IEEE Trans. Biomed. Eng.*, vol. 41, no. 4, pp. 305–313, Apr. 1994.

[10] S. Takeuchi and I. Shimoyama, "A three-dimensional shape memory alloy microelectrode with clipping structure for insect neural recording," *IEEE J. Microelectromech. Syst.*, vol. 9, no. 1, pp. 24–31, Mar. 2000.

[11] T. Suzuki, K. Mabuchi, and S. Takeuchi, "A 3-D flexible parylene probe array for multichannel neural recording," in *Proc. 1st Int. IEEE-EMBS Conf. Neural Engineering*, Capri Island, Italy, Mar. 20–22, 2003, pp. 154–156.

[12] K. Najafi, "Solid-state microsensors for cortical nerve recordings," *IEEE Eng. Med. Bio. Mag.*, vol. 13, no. 3, pp. 375–387, Jun.-Jul. 1994.

[13] H. Eichenbaum, D. Pettijohn, A. M. Delucia, and S. L. Chorover, "Compact miniature microelectrode-telemetry system," *Physiol. Behav.*, vol. 18, pp. 1175–1178, 1977.

[14] C. Pinkwart and H. W. Borchers, "Miniature three-function transmitting system for single neuron recording, wireless brain stimulation, and marking," *J. Neurosci. Meth.*, vol. 20, pp. 341–352, 1987.

[15] A. Nieder, "Miniature stereo radio transmitter for simultaneous recording of multiple single-neuron signals from behaving owls," *J. Neurosci. Meth.*, vol. 101, pp. 157–164, 2000.

[16] S. Takeuchi and I. Shimoyama, "A radio-telemetry system with a shape memory alloy microelectrode for neural recording of freely moving insects," *IEEE Trans. Biomed. Eng.*, vol. 51, no. 1, pp. 133–137, Jan. 2004.

[17] I. Obeid, M. A. L. Nicolelis, and P. D. Wolf, "A multichannel telemetry system for single unit neural recordings," *J. Neurosci. Meth.*, vol. 133, pp. 33–38, 2004.

[18] H. J. Song, D. R. Allee, and K. T. Speed, "Single chip system for bio-data acquisition, digitization, and telemetry," in *Proc. IEEE-ISCAS*, Hong Kong, Jun. 9–12, 1997, pp. 1848–1851.
[19] J. Kim and R. Harjani, "An ISM band CMOS integrated transceiver design for wireless telemetry system," in *Proc. IEEE-ISCAS*, vol. 4, May 6–9, 2001, pp. 694–697.
[20] J. Parramon, P. Doguet, D. Martin, M. Verleyssen, R. Munoz, L. Leija, and E. Valderrama, "ASIC-based batteryless implantable telemetry microsystem for recording purposes," in *Proc. 19th Int. IEEE-EMBS Conf.*, Chicago, IL, Oct. 30–Nov. 2 1997, pp. 2225–2228.
[21] P. Irazoqui-Pastor, I. Mody, and J. W. Judy, "*In vivo* recording using a wireless implantable neural transceiver," in *Proc. 1st Int. IEEE-EMBS Conf. Neural Eng.*, Capri Island, Italy, Mar. 20–22, 2003, pp. 622–625.
[22] G. A. DeMichele and P. R. Troyk, "Integrated multichannel wireless biotelemetry system," in *Proc. 25th Int. IEEE-EMBS Conf.*, Cancun, Mexico, Sep. 17–21, 2003, pp. 3372–3375.
[23] E. A. Johannessen *et al.*, "Implementation of multichannel sensors for remote biomedical measurements in a microsystems format," *IEEE Trans. Biomed. Eng.*, vol. 51, no. 3, pp. 525–535, Mar. 2004.
[24] H. Yu, R. H. Olsson, K. D. Wise, and K. Najafi, "A wireless microsystem for multichannel neural recording microprobes," in *Proc. Solid-State Sensor Actuator Microsystems Workshop*, Hilton-Head Island, SC, Jun. 6–10, 2004, pp. 107–110.
[25] M. Mojarradi, D. Brinkley, B. Blalock, R. Anderson, N. Ulshoefer, T. Johnson, and L. D. Castillo, "A miniaturized neuroprosthesis suitable for implantation into the brain," *IEEE Trans. Neural. Syst. Rehab. Eng.*, vol. 11, no. 1, pp. 38–42, Mar. 2003.
[26] P. Mohseni and K. Najafi, "Wireless multichannel biopotential recording using an integrated FM telemetry circuit," in *Proc. 26th Annu. Int. IEEE-EMBS Conf.*, San Francisco, CA, Sep. 1–5, 2004, pp. 4083–4086.
[27] ——, "A fully integrated neural recording amplifier with DC input stabilization," *IEEE Trans. Biomed. Eng.*, vol. 51, no. 5, pp. 832–837, May 2004.
[28] ——, "A 1.48-mW low-phase-noise analog frequency modulator for wireless biotelemetry," *IEEE Trans. Biomed. Eng.*, vol. 52, no. 5, pp. 938–943, May 2005.
[29] [Online]. Available: http://a257.g.akamaitech.net/7/257/2422/05dec20031700/edocket.access.gpo.gov/cfr_2003/octqtr/pdf/47cfr15.239.pdf
[30] S. A. Nikles, D. S. Pellinen, J. Kitagawa, R. M. Bradley, D. R. Kipke, and K. Najafi, "Long term *in vitro* monitoring of polyimide microprobe electrical properties," in *Proc. 25th Annu. Int. IEEE-EMBS Conf.*, Cancun, Mexico, Sep. 17–21, 2003, pp. 3340–3343.
[31] *Passive Multichannel Recording and Stimulating Electrode Arrays: A Catalog of Available Designs*, Center for Neural Communication Technology, Univ. Michigan, Ann Arbor, 1999, pp. 1–6.
[32] X. Wang, "On cortical coding of vocal communication sounds in primates," in *Proc. Natl. Acad. Sci.*, vol. 97, 2000, pp. 11 843–11 849.

Pedram Mohseni (S'94–M'05) was born in 1974. He received the B.S. degree in electrical engineering from Sharif University of Technology, Tehran, Iran, in 1996 and the M.S. and Ph.D. degrees in electrical engineering from the University of Michigan, Ann Arbor, in 1999 and 2005, respectively.

From June 1998 to December 1998, he was with Canopus Systems Inc., Ann Arbor, MI, developing signal processing algorithms for the multistage decimation and filtering of highly oversampled outputs of sigma-delta converters in a closed-loop microgravity microaccelerometer system. During 2000–2005, he was with the Center for Wireless Integrated MicroSystems (WIMS), University of Michigan. He joined the Faculty of Electrical Engineering and Computer Science Department, Case Western Reserve University, Cleveland, OH, as a tenure-track Assistant Professor in August 2005. His research interests include analog/mixed-signal/RF integrated circuits and microsystems for neural engineering, low-power wireless sensing/actuating systems, biomedical microtelemetry, and assembly/packaging of biomicrosystems. He has authored eight papers in refereed IEEE journals and conferences.

Dr. Mohseni has served as a technical reviewer for the IEEE JOURNAL OF SOLID-STATE CIRCUITS, IEEE TRANSACTIONS ON BIOMEDICAL ENGINEERING, IEEE TRANSACTIONS ON CIRCUITS AND SYSTEMS, and IEEE SENSORS JOURNAL since 2002. He is a member of the IEEE Solid-State Circuits and the IEEE Engineering in Medicine and Biology societies.

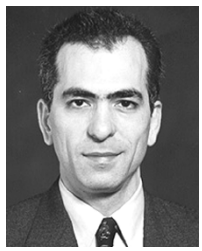

Khalil Najafi (S'84–M'86–SM'97–F'00) was born in 1958. He received the B.S., M.S., and Ph.D. degrees in electrical engineering from the Department of Electrical Engineering and Computer Science, University of Michigan, Ann Arbor, in 1980, 1981, and 1986, respectively.

From 1986 to 1988, he was a Research Fellow, from 1988 to 1990 an Assistant Research Scientist; from 1990 to 1993 an Assistant Professor; from 1993 to 1998 an Associate Professor; and since September 1998, a Professor and the Director of the Solid-State Electronics Laboratory, Department of Electrical Engineering and Computer Science, University of Michigan. His research interests include micromachining technologies, micromachined sensors, actuators, and MEMS; analog integrated circuits; implantable biomedical microsystems; micropackaging; and low-power wireless sensing/actuating systems. He has been active in the field of solid-state sensors and actuators for more than 20 years, and has been involved in several conferences and workshops dealing with solid-state sensors and actuators, including the International Conference on Solid-State Sensors and Actuators, the Hilton-Head Solid-State Sensors and Actuators Workshop, and the IEEE/ASME Micro Electromechanical Systems (MEMS) Conference. He is an Associate Editor for the *Journal of Micromechanics and Microengineering*, Institute of Physics Publishing and an Editor for the *Journal of Sensors and Materials*.

Dr. Najafi was awarded a National Science Foundation Young Investigator Award from 1992 to 1997, was the recipient of the Beatrice Winner Award for Editorial Excellence at the 1986 International Solid-State Circuits Conference of the Paul Rappaport Award for co-authoring the Best Paper published in the IEEE TRANSACTIONS ON ELECTRON DEVICES, and of the Best Paper Award at ISSCC 1999. In 2003, he received the EECS Outstanding Achievement Award, in 2001 he received the Faculty recognition Award, and in 1994 the University of Michigan's "Henry Russel Award" for outstanding achievement and scholarship, and was selected as the "Professor of the Year" in 1993. In 1998, he was named the Arthur F. Thurnau Professor for outstanding contributions to teaching and research, and received the College of Engineering's Research Excellence Award. He is the editor for Solid-State Sensors for IEEE TRANSACTIONS ON ELECTRON DEVICES. He also served as the Associate Editor for IEEE JOURNAL OF SOLID-STATE CIRCUITS from 2000 to 2004, and the Associate Editor for IEEE TRANSACTIONS ON BIOMEDICAL ENGINEERING from 1999 to 2000.

Steven J. Eliades was born in 1977. He received the B.S. degree in biomedical engineering from The Johns Hopkins University, Baltimore, MD, in 1999. He is currently working toward the M.D. and Ph.D. degrees at Johns Hopkins School of Medicine, Baltimore.

Since 2000, he has been with the Laboratory of Auditory Neurophysiology, Department of Biomedical Engineering, Johns Hopkins School of Medicine. His research interests include neural mechanisms of sound perception, structure and function of the auditory cortex, neural basis of primate vocal communication and behavior, sensory-motor interactions in the auditory system, and multielectrode technologies for neurophysiology in free-roaming animals. He has authored two papers in peer-reviewed neuroscience journals.

Dr. Eliades received the Sommerman Graduate Teaching Assistant Award from the Whiting School of Engineering, Johns Hopkins University, in 2002.

Xiaoqin Wang (M'97) received the B.S. degree in electrical engineering from Sichuan University, Chengdu, China, in 1984, the M.S.E. degree in electrical engineering and computer science from University of Michigan, Ann Arbor, in 1986, and the Ph.D. degree in biomedical engineering from The Johns Hopkins University, Baltimore, MD, in 1991.

From 1992 to 1995, he conducted postdoctoral research in somatosensory and auditory neuroscience at University of California, San Francisco. He joined the faculty of Biomedical Engineering Department, Johns Hopkins University School of Medicine, Baltimore, MD, in 1995 and is currently an Associate Professor of biomedical engineering and neuroscience. His research interests range from auditory neurophysiology to neural engineering and include structures and functions of the auditory cortex, neural coding mechanisms, neural mechanisms underlying vocal communication, and computational models of auditory and vocal processing in the brain. He directs the Laboratory of Auditory Neurophysiology in the Department of Biomedical Engineering, Johns Hopkins University.

Dr. Wang received a U.S. Presidential Early Career Award for Scientists and Engineers (PECASE) in 1999 and was the recipient of a Kleberg Foundation postdoctoral fellowship in 1992.